GEOLOGICA CARPATHICA, APRIL 2007, 58, 2, 169–179

Igneous rock clasts from the Maastrichtian Bovec flysch (Slovenia): petrology and geodynamic aspects

ANGELO DE MIN[1], ALBERTO ROSSET[1], GIORGIO TUNIS[2], CRISTINA KOCMANN[3], ALESSANDRO TOSONE[1] and DAVIDE LENAZ[1]

[1]Dipartimento di Scienze della Terra, via Weiss 8, 34127 Trieste, Italy; demin@univ.trieste.it
[2]Dipartimento di Scienze Geologiche, Ambientali e Marine, via Weiss 2, 34127 Trieste, Italy
[3]Hydrotech S.r.l. — AREA Science Park, Padriciano 99, 34012 Trieste, Italy

(Manuscript received January 13, 2006; accepted in revised form October 5, 2006)

Abstract: About sixty well sorted (average diameter 0.8 cm) volcanic clasts with tholeiitic affinities were found in the midst of an lower Maastrichtian conglomerate outcropping close to Bovec (Slovenian Basin, NW Slovenia) and interpreted as evidence of a deltaic system. The clasts appear to be variably spilitized (i.e. albitization of plagioclase and anomalous Na content), however, they do not show any evidence of sub-solidus recrystallization. The analysis, carried out on nineteen selected samples, point out similar petrographic textures and a strong arc-type chemical signature (i.e. deep Nb negative anomaly, quite low La/Sm and Th/Zr ratio and normative corundum). Chemical data allow us to distinguish, for comparable grade of evolution, variable LREE contents which cannot be related only to crystal fractionation or to a variable grade of crustal contamination, but require compositional differences in the protolithic sources. To have an indication of the provenance of these clasts, and about their related hydrographic system, their chemical features were compared to those of similarly evolved pre-Maastrichtian magmatic rocks of different ages, locations and geological settings, mainly belonging to the Dinaridic-Carpathian region. Such a comparison seems to indicate a particular affinity with the arc-type magmas which outcropped in the Vardar Ocean in Jurassic times. In particular Bovec clasts show strong chemical similarities with metabasites from the ophiolitic complexes of the Evros (Rhodopes) and Vardar Zone, while they appear quite different from both the more depleted samples from Bükk Mountains (Hungary), and all the calc-alkaline compositions considered. The grain size of the clasts and the complete absence of recrystallization suggest a provenance from a quite delimited and close protolithic area (1–3 hundred kilometers) that did not suffer from sub-solidus recrystallization during Late Cretaceous times.

Key words: Maastrichtian, Bovec (NW Slovenia), Vardar Zone, sedimentary petrology, conglomerates, arc-type tholeiitic clasts.

Introduction

Traditional provenance studies investigate the large-scale geodynamic framework of ancient geological setting and infer the types of eroded rocks which supplied clastic systems in order to improve our knowledge of paleogeography. Thus they could successfully identify the rock types which sourced a certain clastic body, and finally their paleogeographical location, by combining petrologic data with basin analysis studies. A comparison of the geochemical data from pebbles of the flysch and potential source rocks will help to elucidate the flysch provenance.

In this way, the conglomerates of the Bovec Basin (part of Slovenian Basin), which probably represents a branch in the evolution of the Pindos Sea at this latitude during early Maastrichtian times, appears related to a not extended hydrographic basin and associated with the development of an orogenic wedge. Moreover, the deposits of the inner margin of the Slovenian Basin are rarely observed: the lower Maastrichtian conglomerates outcropping near Bovec, represent a significant exception.

Thus, the chemical features of the clasts and the present day Peri-Tethys plate reconstruction models could provide an important clue both to define the protolithic areas and to insert the Bovec sector of the Slovenian Basin within the geodynamic evolution of the Alpidic-Dinaric and Carpathian domains.

Geology and stratigraphy

The studied area (Fig. 1) is located inside the Bovec sedimentary basin, situated between Mt Rombon and Mt Polovnik structural highs (NW Slovenia; Fig. 2) close to Bovec village. The oldest terrains (Fig. 2) of the stratigraphic succession belong to the Julian Carbonate Platform (Buser 1986a,b), and are represented by Norian and Rethyan limestones to dolostones (*Dachstein* and *Main Dolomite* formations), which are interpreted as peritidal carbonates. Early-Middle Jurassic is represented by oolithic limestones and minor carbonate breccias (Buser 1986a) testifying to the presence of a shallow sea (carbonate ramp) and short-lasting periods of emersion of the carbonate platform, respectively (Selli 1947). From the Dogger, the Julian Carbonate Platform was eroded (Buser 1986a,b) due to compressive NE-SW trending faults which led to the folding of the area (Selli 1947), and to the raising of a deep marine plateau, now represented by Mt Rombon and

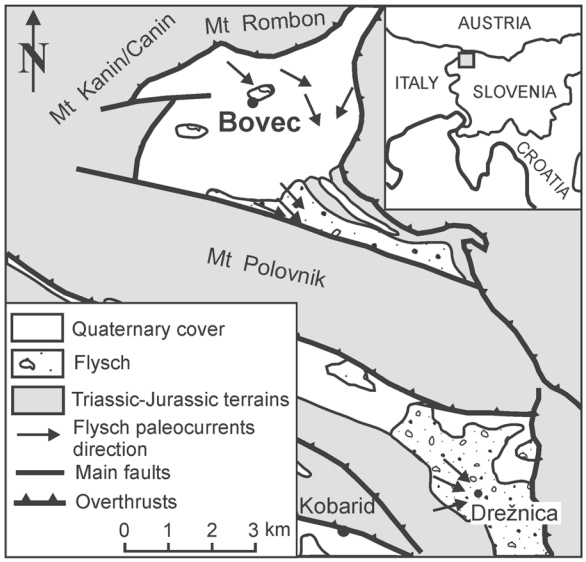

Fig. 1. Geological sketch map of the studied area showing the flysch outcrops (modified after Kuščer et al. 1974 and Buser 1986a,b). Inset: Geographical location of Bovec Basin.

Mt Polovnik highs (Fig. 2). Due to this tectonic event, the Mt Polovnik high acted as a partition between two small distinct deep-water sub-basins, known in literature as Bovec and Kobarid sub-basins (Kuščer et al. 1974).

The Cretaceous deposits of the Bovec area include reddish marly limestone and marl with chert (Scaglia Rossa Formation) and grey marly limestone with chert (Volče limestone) which are interpreted as thin-bedded calciturbidites (Ogorelec et al. 1976). These turbidites, deposited during the Campanian (Pavšič 1994), are linked to the beginning of a new tectonic phase which is traditionally related to the Ressen compressive phase (Kuščer et al. 1974). Calci-turbiditic clasts mostly derived from resedimented shallow marine carbonates (i.e. Friuli Carbonate Platform) situated at the outer side of the Slovenian Basin. Successively, during the Maastrichtian, a gradually increasing input of terrigenous material, started in the Bovec area (Kuščer et al. 1974) so that a gradual variation from a calciclastic deep-water system to a siliciclastic one occurred.

Conglomerate beds 5–10 meter thick on the whole can be observed about 400 m above the base of the flysch succession. The most common lithologies observed among the clasts of the conglomerates include Mesozoic limestone and dolostone derived both from an inner carbonate platform and plateau areas (see the above mentioned formations), chert, lydites, quartzites, plagioclase-rich and chromite-bearing sandstones (Lenaz et al. 2000), metapelites and scarce unmetamorphosed occasionally spilitized volcanic clasts (Rosset et al. 2003).

According to Selli (1947) and Kuščer et al. (1974), the conglomerates indicate the existence, at that time, of a

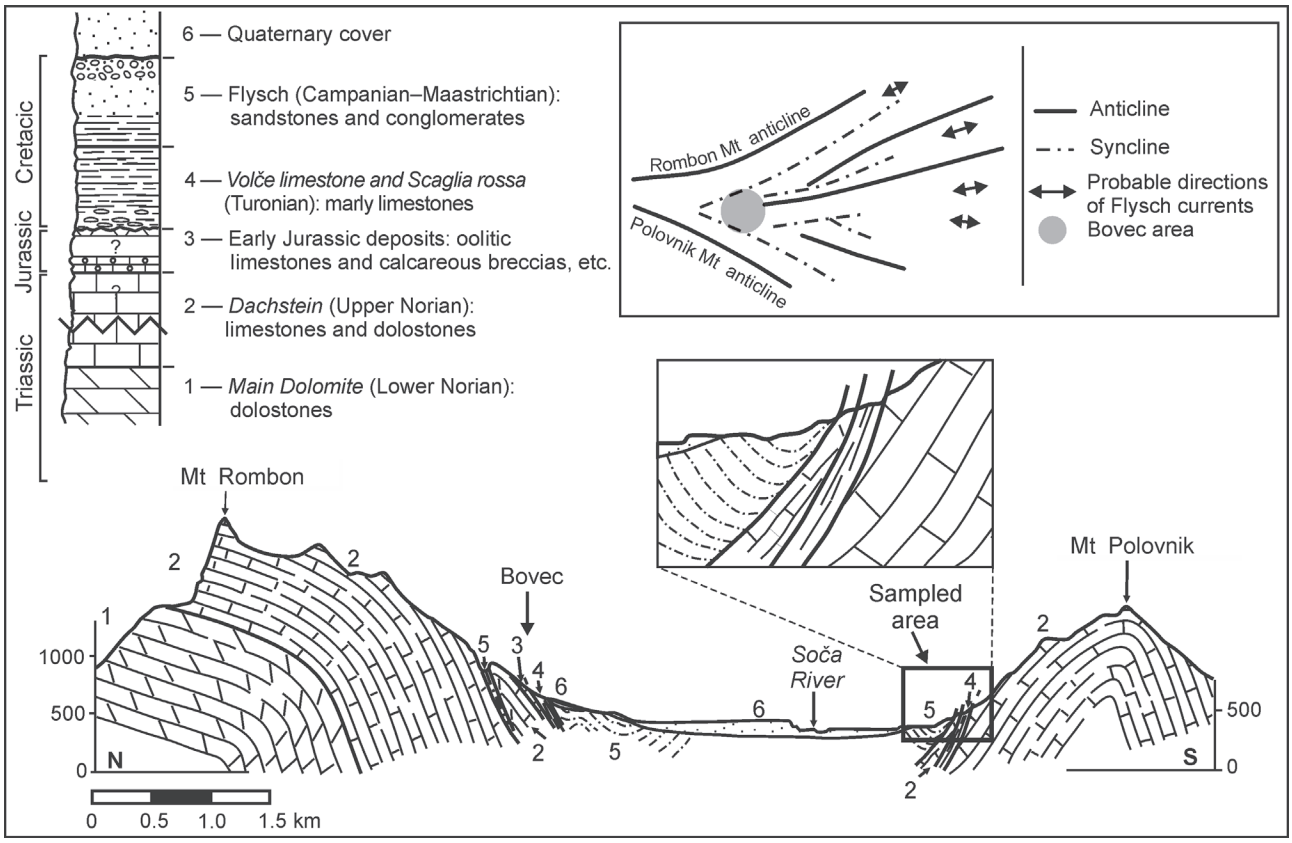

Fig. 2. Stratigraphic column and stratigraphic section of Bovec Basin (modified from Selli 1947). Inset: tectonic settings of the Julian Alps during Late Cretaceous times (modified from Selli 1947).

deltaic system. More probably, these deposits represent a "mixed system" as proposed by Mutti et al. (2003) characterized by an association of immature, turbidite like bodies and deltaic deposits situated at the internal margin of the Slovenian Basin, which was strongly influenced by the proximity of a growing orogen.

Petrography and classification of the clasts

Igneous clasts are quite rare in the Bovec conglomerates and only 69 items have been sampled so far. They have a mean size diameter variable from 0.4 to 2.0 cm (average 0.8 cm) and their shape appear to be compatible with fluvial transport as suggested by Kuščer et al. (1974). In fact, their grain size and the quite high density (about 2.7–2.9 g/cm^3), together with associations with facies typical of immature turbidite, suggest transport by small to medium-sized rivers, presumably characterized by relatively short and high-gradient transfer zones.

Optically, all the volcanic clasts show intersertal and/or micro-porphyritic textures. Rare pheno- and microphenocrystals of plagioclase, augite, pigeonite and opaques have been observed. Olivine, completely altered into iddingsitic products appears to be occasional. Microlites are quite abundant and mainly represented by albitized plagioclase and clinopyroxene. Secondary mineral phases are represented by carbonates such as plagues inside plagioclase and/or inside glass, and by scarce zeolites filling micro-fractures and very rare vacuoles. Glass is very abundant and partially recrystallized into clay minerals. In general, due to their mineralogical assemblage the clasts

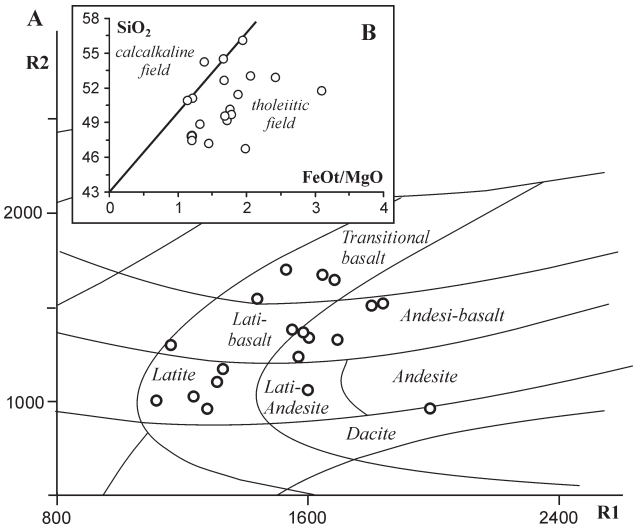

Fig. 3. A — Distribution of the Bovec volcanic clasts in R1-R2 classification diagram of De La Roche et al. (1980) as modified by Bellieni et al. (1981). **B** — SiO_2 vs. FeO_t/MgO diagram for basic sub-alkaline rocks (Miyashiro 1974).

Table 1: Microprobe compositions of pyroxenes of the Bovec volcanic clasts. E and L — early and late crystallized pyroxene. Aug — augite; Pig — pigeonite. Fe^{3+} calculated according to Papike et al. (1974); Fe* = Fe^{2+}+Mn+Fe^{3+}.

	BV28		BV32							BV33				
	E Aug	L Aug	E Aug	L Aug	E Aug	E Aug	L Aug	L Pig	L Pig	E Aug	E Aug	E Aug	E Aug	E Aug
SiO_2 (wt.%)	53.22	52.78	52.49	51.33	52.78	51.22	51.78	50.43	50.22	51.08	50.56	51.22	51.23	51.60
TiO_2	0.47	0.56	0.62	0.58	0.56	0.78	0.82	0.42	0.32	0.92	0.91	0.84	0.82	0.72
Al_2O_3	2.11	2.09	1.86	1.90	2.12	2.59	2.67	1.61	1.72	1.93	2.21	2.05	2.09	1.68
FeO_{total}	6.95	7.70	8.01	7.80	7.43	8.03	8.30	22.94	22.85	12.14	10.80	11.18	10.03	11.68
MnO	0.20	0.25	0.23	0.22	0.25	0.20	0.31	0.41	0.39	0.36	0.30	0.38	0.32	0.37
MgO	16.95	17.06	16.64	16.16	16.57	15.93	16.11	16.75	17.01	14.41	14.71	14.51	14.95	14.74
CaO	20.38	19.86	20.27	20.33	20.30	20.01	20.25	6.42	6.50	19.36	19.71	19.69	19.84	19.30
Na_2O	0.20	0.23	0.24	0.21	0.23	0.27	0.29	0.89	0.93	0.28	0.28	0.31	0.29	0.30
K_2O	0.02	0.01	0.02	0.02	0.00	0.00	0.02	0.09	0.01	0.01	0.01	0.01	0.00	0.00
Cr_2O_3	0.07	0.17	0.06	0.06	0.11	0.10	0.05	0.04	0.05	0.07	0.02	0.00	0.07	0.00
Sum	100.57	100.71	100.44	98.61	100.34	99.12	100.60	100.00	100.00	100.56	99.51	100.20	99.63	100.40
Si (a.p.f.u.)	1.942	1.932	1.924	1.918	1.935	1.914	1.899	1.905	1.893	1.904	1.894	1.910	1.913	1.920
Al^{IV}	0.058	0.068	0.076	0.082	0.065	0.086	0.101	0.072	0.076	0.085	0.098	0.090	0.087	0.070
Sum	2.000	2.000	2.000	2.000	2.000	2.000	2.000	2.000	2.000	1.989	1.992	2.000	2.000	1.990
Al	0.033	0.022	0.004	0.002	0.027	0.028	0.014	0.000	0.000	0.000	0.000	0.000	0.005	0.000
Fe^{2+}	0.200	0.208	0.193	0.180	0.207	0.221	0.192	0.561	0.561	0.303	0.256	0.282	0.258	0.300
Fe^{3+}	0.012	0.028	0.053	0.063	0.021	0.030	0.062	0.163	0.163	0.075	0.082	0.066	0.055	0.070
Cr^{3+}	0.002	0.005	0.002	0.002	0.003	0.003	0.001	0.001	0.001	0.002	0.001	0.000	0.002	0.000
Mg	0.922	0.931	0.909	0.900	0.906	0.869	0.881	0.943	0.956	0.801	0.822	0.807	0.832	0.820
Mn	0.006	0.008	0.007	0.007	0.008	0.006	0.010	0.013	0.012	0.011	0.010	0.012	0.010	0.012
Ti	0.013	0.015	0.017	0.016	0.015	0.022	0.023	0.012	0.009	0.026	0.026	0.024	0.023	0.020
Ca	0.797	0.767	0.796	0.814	0.797	0.801	0.795	0.260	0.263	0.773	0.791	0.787	0.794	0.770
Na	0.014	0.016	0.017	0.015	0.016	0.020	0.021	0.065	0.068	0.020	0.020	0.022	0.021	0.022
K	1.999	2.000	1.998	1.999	2.000	2.000	1.999	2.022	2.033	2.011	2.008	2.000	2.000	2.014
Sum	1.999	2.000	1.998	1.999	2.000	2.000	1.999	2.018	2.033	2.011	2.008	2.000	2.000	2.014
Ca (at.%)	41.15	39.50	40.65	41.45	41.10	41.57	40.98	13.40	13.45	39.38	40.34	40.28	40.74	39.05
Mg	47.60	47.94	46.42	45.82	46.73	45.10	45.41	48.61	48.90	40.80	41.92	41.30	42.69	41.58
Fe*	11.25	12.56	12.92	12.73	12.17	13.34	13.61	37.99	37.65	19.82	17.75	18.42	16.57	19.37
T (°C)	–	–	–	1060	–	–	1067	–	–	–	–	–	–	–

appear to be tholeiitic basalts, andesitic basalts and transitional-basalts with tholeiitic affinity (i.e. coexistence of quite altered olivine and pigeonite). Moreover, the petrographic features indicate an effusive or sub-effusive origin characterized by a rapid quench. The coexistence of albitized and Ca-rich plagioclase suggests spilitization processes. On a petrographical basis, nineteen quite fresh samples were selected, analysed for major elements and plotted (Fig. 3A) in the R1-R2 classification diagram of De La Roche et al. (1980) as modified by Bellieni et al. (1981), here preferred to the most common TAS (*Total Alkali Silica;* Le Bas et al. 1986) because it gives clear petrographic evidence of Na mobilization. The samples, in agreement with the optical features, plot in the transitional and sub-alkaline fields, from transitional- and andesi-basalt to latites and lati-andesites. The tholeiitic affinity is supported by the SiO_2 vs. FeO_t/MgO diagram of Miyashiro (1974; Fig. 3B), in which most of the samples fall in the tholeiitic field; only a few samples fall between the tholeiitic and the calc-alkaline fields and only one sample falls in the calc-alkaline one. Finally, most samples are both Q and C normative.

Mineral chemistry

Microprobe analyses were carried out on the largest samples (∅>1 cm; BV17, BV28, BV32 and BV33) using a Cameca–Camebax operating at 15 kV and 15 nA, at the Dipartimento di Mineralogia e Petrologia, University of Padova (Italy). The PAP Cameca program has been used to convert X-ray counts into weight percent of the corresponding oxides. Results are considered accurate within 2–3 % for major elements and 9 % for minor elements.

The analysed **pyroxenes** (Table 1) are mainly represented by micro-phenocrysts of augite (Wo_{39-42} En_{41-48} Fs_{11-20}) quite homogeneous in composition, which plot over the Skaergaard trend (Brown & Vincent 1963). The rare un-altered associate pigeonites (Wo_{13} En_{48-49} Fs_{37-38}) confirm the tholeiitic affinity of these rocks. Kretz's (1982) crystallization temperature of late-crystallized augite, obtained for sample BV32, yielded values of 1060–1067 °C.

Feldspar microprobe compositions (Table 2) show two main feldspar groups in agreement with the optical features. They are represented by albite-oligoclase (An_{0-13};

Table 2: Microprobe plagioclase compositions of the Bovec volcanic clasts. E and L — early and late crystallized plagioclase. Or, Ab and An — orthoclase, albite and anorthite, respectively. Crystallization temperatures (T °C) were obtained using the geothermometer of Kudo & Weill (1970).

a	BV32						BV17					
	E	E	E	E	E	E	L	E	E	L	L	E
SiO_2	57.00	53.48	55.31	57.86	53.62	59.87	70.06	68.26	67.97	68.75	69.05	68.22
TiO_2	0.02	0.07	0.07	0.06	0.12	0.05	0.01	0.03	0.02	0.01	0.02	0.03
Al_2O_3	26.82	28.91	27.59	26.35	28.41	25.19	20.30	20.51	20.35	20.08	20.09	20.38
FeO_{total}	0.79	0.93	1.08	0.75	0.85	0.49	0.16	0.15	0.32	0.20	0.20	0.18
MnO	0.02	0.00	0.00	0.01	0.00	0.00	0.01	0.06	0.02	0.04	0.01	0.01
MgO	0.07	0.11	0.07	0.06	0.12	0.02	0.01	0.03	0.02	0.01	0.01	0.01
CaO	9.84	12.22	11.05	9.21	12.00	7.51	0.10	0.69	0.57	0.06	0.13	0.15
K_2O	0.12	0.14	0.05	0.05	0.25	0.16	9.29	10.85	10.64	10.86	11.21	10.82
Na_2O	6.01	4.52	5.36	6.20	4.29	7.42	0.07	0.14	0.10	0.06	0.07	0.16
Sum	100.70	100.37	100.58	100.54	99.67	100.70	100.03	100.72	100.00	100.08	100.80	99.99
Ab (wt.%)	50.66	48.16	45.14	49.26	41.74	54.66	98.56	97.05	96.53	97.43	98.95	85.86
An	48.64	51.09	54.58	50.42	56.85	44.22	0.86	2.14	2.93	1.94	0.67	13.26
Or	0.70	0.75	0.28	0.31	1.41	1.12	0.58	0.81	0.53	0.62	0.38	0.88
T (°C)												
Dry	1373	1385	1401	1360	1439	1312	–	–	–	–	–	–
50 MPa	1446	1458	1474	1434	1511	1387	–	–	–	–	–	–
100 MPa	1427	1439	1455	1415	1492	1367	–	–	–	–	–	–
500 MPa	1295	1308	1325	1283	1363	1232	–	–	–	–	–	–

b	BV33			BV28						
	E	E	E	E	E	E	L	E	L	E
SiO_2	50.42	57.71	59.44	68.95	68.80	65.84	69.19	69.77	68.63	67.46
TiO_2	0.05	0.04	0.06	0.00	0.00	0.04	0.00	0.00	0.01	0.05
Al_2O_3	30.40	25.87	25.40	19.95	20.32	19.76	20.41	20.32	20.92	19.73
FeO_{total}	0.57	0.52	0.58	0.24	0.16	1.42	0.15	0.15	0.17	0.10
MnO	0.05	0.02	0.00	0.00	0.00	0.07	0.00	0.01	0.00	0.01
MgO	0.18	0.04	0.02	0.00	0.01	0.43	0.00	0.02	0.00	0.00
CaO	14.58	8.89	7.97	0.38	0.75	0.44	0.29	0.16	0.96	0.85
K_2O	0.02	0.10	0.20	0.06	0.00	0.27	11.30	10.90	9.27	11.14
Na_2O	3.23	6.49	6.91	11.09	10.97	10.44	0.06	0.03	0.01	0.04
Sum	99.50	99.67	100.57	100.67	101.01	98.72	101.39	101.37	99.98	99.38
Ab (wt.%)	38.09	50.30	52.58	95.22	92.34	95.91	99.03	98.15	98.96	94.23
An	61.81	49.04	46.06	4.04	7.66	2.37	0.44	1.49	0.84	5.71
Or	0.11	0.66	1.36	0.74	0.00	1.72	0.53	0.36	0.20	0.06
T (°C)										
Dry	1283	1130	1107	–	–	–	–	–	–	–
50 MPa	1352	1207	1185	–	–	–	–	–	–	–
100 MPa	1335	1187	1165	–	–	–	–	–	–	–
500 MPa	1211	1048	1024	–	–	–	–	–	–	–

average An_3) and plagioclase with anorthitic contents ranging from An_{44} to An_{62} (average An_{52}). The first group is represented by spilitized plagioclases, while the other appears to be quite compatible with the evolution degree of the rocks (Mg#=0.4–0.6; Mg#=[Mg]/[Mg+Fe^{2+}] for Fe_2O_3/FeO=0.15). Temperatures of 1024 and 1048 ºC, comparable with those of pyroxenes, were obtained on two anorthitic plagioclase belonging to sample BV33 by using the geothermometer of Kudo & Weill (1970) and assuming a P_{H2O} = 500 MPa. In the same clast a Ca-rich plagioclase (An_{62}) gave a higher temperature of 1211 ºC.

The microprobe analyses indicate that **opaques and olivine** are completely transformed respectively into colloidal hydroxides and iddingsite.

Geochemistry

Major and trace elements were determined at the Dipartimento di Scienze della Terra, University of Trieste, by using a PW-1404 XRF spectrometer and the procedures of Philips® for the correction of matrix effects. Major element abundances were recalculated to 100 % on a volatile-free basis. The analytical uncertainties are estimated at less than 2 and 5 % for major and trace elements, respectively. REE (as well as all the trace elements) determinations in the samples BV17 and BV33 were carried out by ICP-MS at the Centre de Recherches Petrographiques et Geochimiques, CNRS, Vandoeuvre (France), and the analytical uncertainties are estimated between 5 and 10 % (Govindaraju & Mevelle 1987).

Major elements

Despite the clastic nature of the volcanics, the most abundant major elements (Table 3, Fig. 4) show broad correlation with SiO_2, here used as a possible evolution index, and indicate a provenance from variably evolved magmatic rocks. Moreover, the decrease of MgO, CaO and FeOt, together with a poor Al_2O_3 increase, shows that a general gabbroic fractionation (olivine, pyroxene and plagioclase) from similar parental melts may have played a role in the genesis of the single protolithes. The evident positive correlation shown by Na_2O, unlike the one shown by K_2O, is here interpreted as a consequence of the albitization processes that occurred during spilitization.

Trace elements

In the Log-Log diagrams (Fig. 4), LREE (for example La) for comparable SiO_2 contents, point out two groups, defined LL (low in LREE) and HL (high in LREE). Such characteristics are not shown by High Field Strength Elements (HFSE) such as Zr, whose concentration in the primary parental melts of the LL and HL groups are comparable. The different behaviour of LREE and some

Table 3: Major (wt. %) and trace (ppm) element contents of the Bovec volcanic clasts. Major elements recalculated to 100 % on a volatile-free basis. PM — Primitive Mantle (La = 0.648 ppm and Nb = 0.658 ppm; McDonough & Sun 1995); $La/Y_{(PM)}$ — La/Y ratio of samples normalized to the Primitive Mantle; HL and LL — samples with $La/Y_{(PM)}$ > and < 3, respectively; **(a)** — values recalculated on Fe_2O_3/FeO ratio of 0.15; Q and C — normative Quartz and Corundum.

	LL group										HL group								
	BO5	**BV28**	**BV29**	**BV30**	**BV32**	**BV33**	**BV34**	**BV56**	**BV66**	**BV67**	**BO2**	**BV17**	**BV31**	**BV49A**	**BV52**	**BV55**	**BV58**	**BV63**	**BV65**
SiO_2 (wt.%)	53.64	52.61	47.16	51.41	51.10	51.72	52.88	46.70	49.66	49.55	47.78	54.90	47.40	48.85	50.91	53.01	56.03	49.16	50.09
TiO_2	2.73	2.08	2.18	2.18	1.46	3.47	2.08	2.26	1.82	2.28	1.37	1.51	2.18	2.10	2.10	2.01	2.24	2.36	2.34
Al_2O_3	20.92	15.84	14.82	17.69	15.86	16.15	16.64	17.34	14.64	15.94	15.07	16.67	14.95	18.15	18.26	15.95	18.58	17.52	17.43
FeO_{total}	6.38	12.02	13.62	12.11	15.32	13.46	10.48	13.21	13.26	15.84	14.49	10.23	14.37	9.98	10.26	12.93	7.03	12.65	12.08
MnO	0.08	0.19	0.53	0.21	0.37	0.27	0.40	0.64	0.31	0.26	0.35	0.13	0.35	0.22	0.16	0.27	0.11	0.30	0.26
MgO	4.13	7.13	9.34	6.41	12.53	4.34	4.31	6.64	7.41	9.40	12.00	6.36	11.90	7.50	8.96	6.25	3.67	7.35	6.83
CaO	6.83	4.81	8.59	5.29	0.27	5.28	7.11	9.67	8.34	2.82	5.99	3.31	5.94	8.58	5.00	3.77	3.88	6.32	6.45
Na_2O	4.66	4.92	1.94	3.53	2.25	4.26	5.32	3.17	3.60	2.98	2.14	5.44	2.12	3.02	3.59	4.86	3.35	3.20	3.31
K_2O	0.32	0.24	1.62	0.95	0.68	0.70	0.58	0.17	0.78	0.63	0.65	1.21	0.64	0.74	0.43	0.70	4.33	0.79	0.78
P_2O_5	0.30	0.16	0.19	0.21	0.16	0.35	0.20	0.20	0.18	0.29	0.15	0.24	0.15	0.86	0.32	0.24	0.77	0.34	0.42
Sum	100.00	100.00	100.00	100.00	100.00	100.00	100.00	100.00	100.00	100.00	100.00	100.00	100.00	100.00	100.00	100.00	100.00	100.00	100.00
FeO (a)	5.62	10.59	12.00	10.67	13.50	11.86	9.23	11.64	11.68	13.96	12.77	9.01	12.66	8.79	9.04	11.39	6.19	11.14	10.64
Fe_2O_3 (a)	0.84	1.59	1.80	1.60	2.02	1.78	1.38	1.75	1.75	2.09	1.92	1.35	1.90	1.32	1.36	1.71	0.93	1.67	1.60
FeOt/MgO	1.54	1.68	1.46	1.89	1.22	3.10	2.43	1.99	1.79	1.69	1.21	1.61	1.21	1.33	1.15	2.07	1.91	1.72	1.77
Q	5.26	3.05	0.97	6.87	16.53	7.63	1.64	0.58	1.33	10.46	2.48	2.68	2.45	1.88	5.11	5.24	8.10	3.85	4.89
C	1.14	0.00	0.00	1.68	11.27	0.00	0.00	0.00	0.00	5.85	0.27	0.91	0.17	0.00	3.49	0.85	2.97	0.63	0.31
Cr (ppm)	141	82	294	154	164	43	91	325	186	83	243	94	243	160	390	116	281	182	177
Ni	57	110	105	113	114	55	64	103	88	107	130	81	130	121	154	87	85	80	79
Ba	269	150	140	400	321	260	278	169	340	198	108	240	514	281	399	209	677	138	116
Rb	29	1	10	14	32	12	8	1	11	5	12	22	12	3	1	6	59	20	15
Sr	162	181	166	227	186	215	179	224	185	333	187	235	187	241	365	161	242	169	147
La	11	15	7	13	7	12	7	10	8	11	26	20	27	32	26	21	29	18	21
Ce	33	45	22	37	21	28	31	34	19	22	54	49	63	71	49	45	59	50	58
Nd	23	26	14	22	16	18	19	18	13	18	33	26	29	49	30	25	27	26	27
Zr	113	88	133	146	101	105	97	148	131	174	98	76	98	145	143	104	143	136	104
Y	26	37	38	38	28	37	28	44	41	43	33	37	33	65	30	31	23	38	42
Nb	1	1	1	1	15	1	1	2	3	1	5	1	5	3	4	1	19	1	1
La/Y_{PM}	2.81	2.69	1.22	2.27	1.66	2.15	1.66	1.51	1.29	1.70	5.23	3.59	5.43	3.27	5.75	4.50	8.37	3.14	3.32

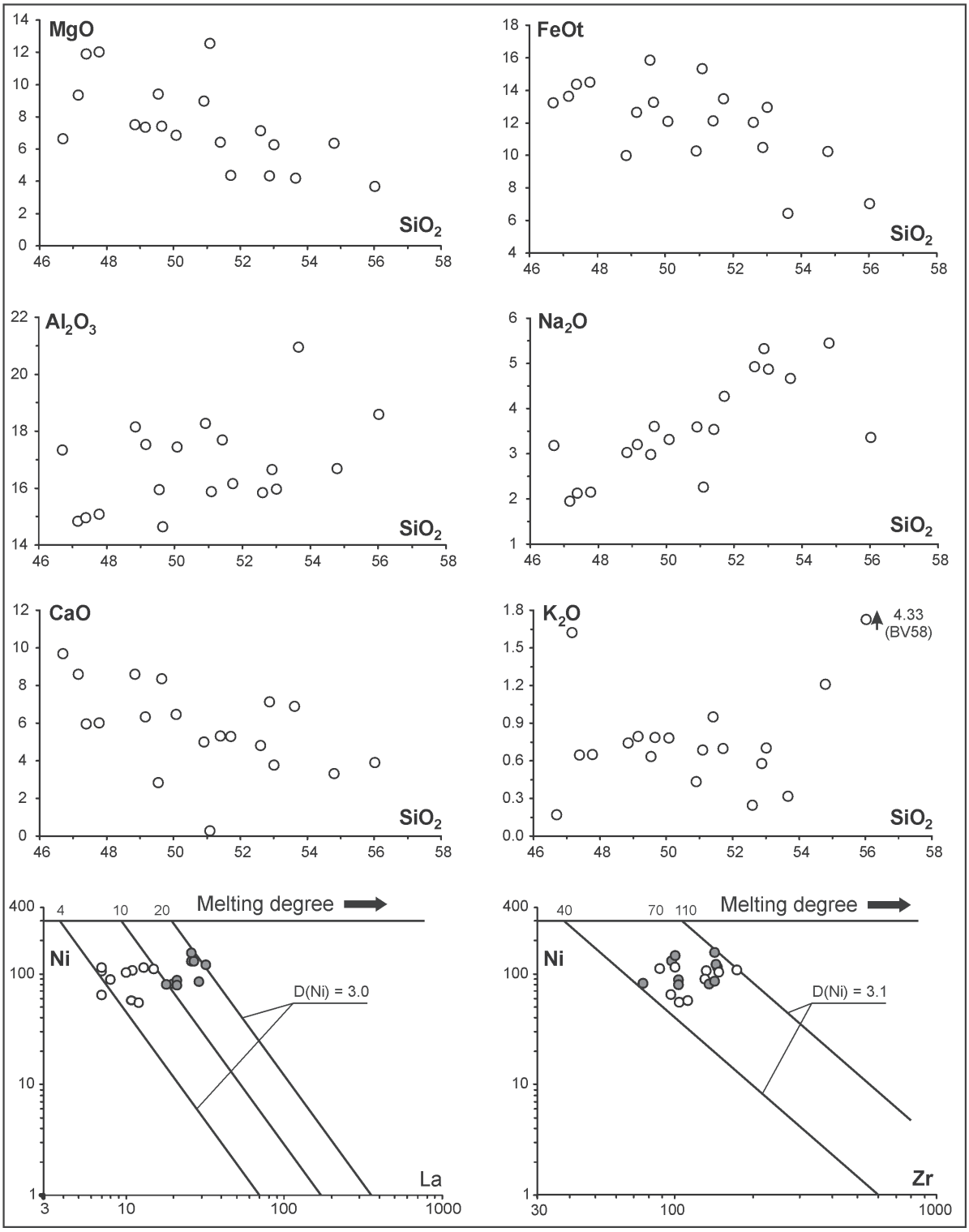

Fig. 4. Major elements (wt. %) vs. SiO_2 variation diagrams of the Bovec volcanic clasts. The Log-Log diagrams of Ni vs. Zr and La show the estimated Zr and La contents of the parental melts of the LL (low in LREE; white circles) and HL (high in LREE; grey circles) volcanic clasts. D — bulk distribution coefficient for Ni.

HFSE vs. Ni cannot be related to a different melting degree or to simple fractionational crystallization (see De Min et al. 2003), but could imply chemical differences in the mantle sources of the protolithic rocks or crustal contamination.

In the multi-elemental diagrams (Fig. 5), both the LL and HL samples are evidence of a deep and comparable negative Nb anomaly (mean Nb/Nb* = 0.10 vs. 0.11, respectively) and similar Large Ion Lithophile Element (LILE) contents. Moreover, a Sr negative anomaly is always

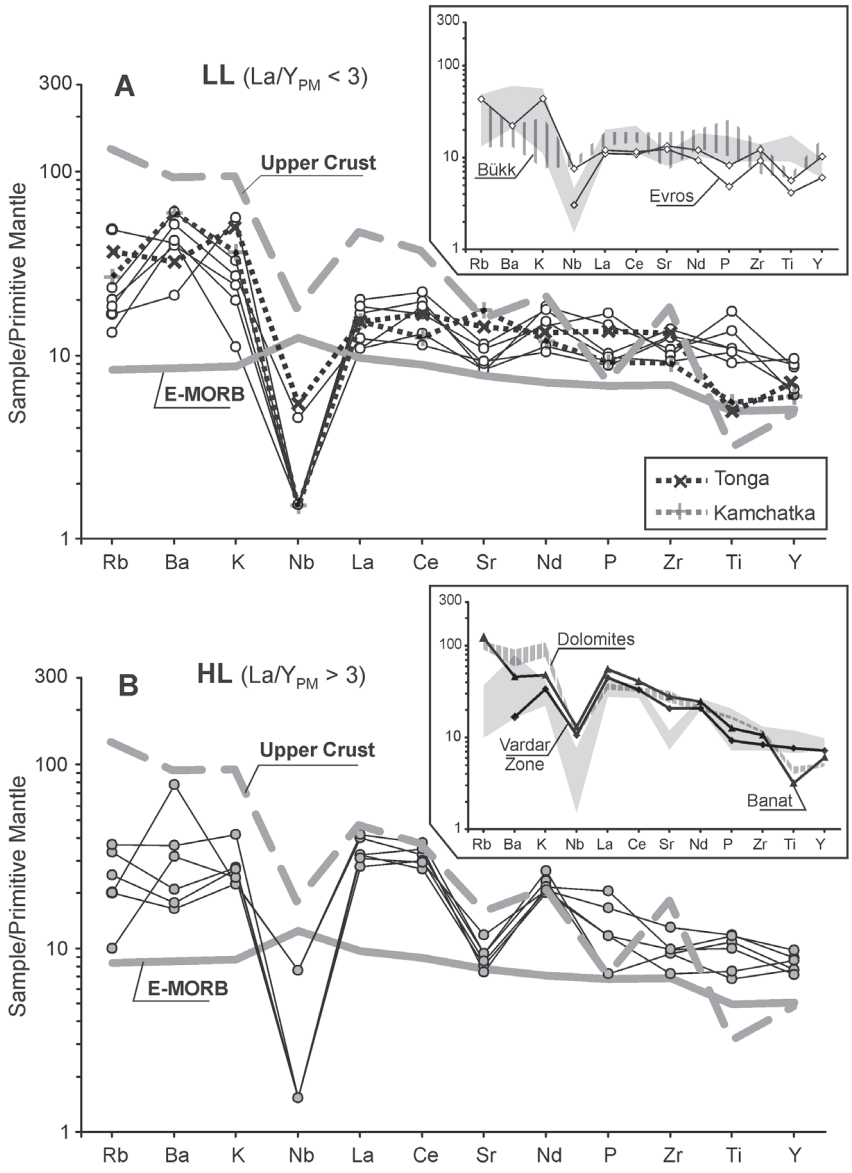

Fig. 5. Incompatible element patterns of Bovec volcanic clasts normalized to Primitive Mantle (PM; McDonough & Sun 1995). **A** — LL samples. E-MORB = Enriched Middle Oceanic Ridge basalt (Sun & McDonough 1989); Kamchatka (Kersting & Arculus 1994); Tonga (Gill 1976). Inset: grey field = LL samples; Bükk (Downes et al. 1990); Evros (Magganas 2002). **B** — HL samples. Upper Crust (Rudnick & Gao 2004). Inset: Dolomites (original data); Banat (Dupont et al. 2002); Vardar Zone (Pamić et al. 2001). Other abbreviations as in Fig. 4.

present to indicate that a variable plagioclase fractionation occurred.

The LL samples are characterized by a flat La to Y pattern with a La/Y$_{PM}$ (Primitive Mantle normalized; McDonough & Sun 1995) ratio (La/Y$_{PM}$=1.5 to 2.8; Fig. 5A) comparable with the E-MORB one (La/Y$_{PM}$=1.9; Sun & McDonough 1989), to suggest a depleted component in the mantle source. Moreover, a strong similarity with arc-type basalts (i.e. Tonga — Gill 1976; Kamchatka — Kersting & Arculus 1994) is strongly supported by the LILE pattern, the comparable Nb anomaly (mean Nb/Nb*=0.10 vs. 0.11 and 0.06, respectively) and by the similar La/Y$_{PM}$ ratio (1.9 vs. 1.7 and 2.6). Conversely, the HL group shows a higher La/Y$_{PM}$ ratio (La/Y$_{PM}$=3.14 to 8.37; Fig. 5B), and its La-Y pattern approaches the Upper Crust one (La/Y$_{PM}$=9.8; Rudnick & Gao 2004).

To define possible provenance constraints, the studied igneous clasts have also been compared with several metabasites from the Vardar Zone (Pamić et al. 2001), Rhodope (Evros; Magganas 2002) and Bükk (Downes et al. 1990) areas (see insets of Fig. 5A,B). Furthermore, to evaluate whether a few samples could belong to a calc-alkaline suite, Triassic and Cretaceous calc-alkaline samples from the Dolomites (unpublished data) and Pannonian Basin (Banat; Dupont et al. 2002) have also been considered for comparison.

It must be pointed out that only the samples which best approach the chemical features of the studied clasts have been selected from each locality.

Among all the possible protoliths, the LL tholeiites (inset of Fig. 5A) show similarities with the less depleted samples from Evros and Bükk (La/Y$_{PM}$=1.1–2.0 and 1.2–1.3, respectively), Ti contents excepted. On the contrary, the HL tholeiites well approach the pattern of the Vardar Zone selected magma (La/Y$_{PM}$=6.21; inset of Fig. 5B), and more generally, they show a better affinity with all the proposed samples with a calc-alkaline signature. It should be noted that from all the considered patterns, only the Vardar Zone magma and Bovec volcanic clasts do not show a TiO_2 negative anomaly (Ti/Ti* values higher than one).

Rare Earth elements

Due to the scarcity of material, only one sample per group (BV33 for LL and BV17 for HL) has been analysed for REE contents (Table 4); these are characterized by quite different La/Yb$_{CN}$ (chondrite normalized; Boynton 1984) ratios (1.8 and 3.1, respectively). The Eu/Eu* ratio approaches 1 for both the samples showing a quite low evolution. In Fig. 6A inset, the selected samples, particularly LL, show both E-MORB-like (La/Yb$_{CN}$=1.8) and arc-type lavas (Tonga; La/Yb$_{CN}$=2.0) signatures, while they strongly differ from the Upper Crust (La/Yb$_{CN}$=10.5). Notably (Fig. 6A), the calc-alkaline magmas from Banat and Dolomites, with an incompatible element pattern recalling those of the HL samples, highlight an Upper Crust-like

Table 4: Rare Earth Element (REE) and Th contents (ppm) of the Bovec volcanic clasts. CN — chondrite normalized (Boynton 1984).

Sample	BV17	BV33
La (ppm)	12.67	8.60
Ce	32.19	22.47
Pr	18.75	14.59
Nd	4.91	4.42
Sm	1.67	1.56
Eu	5.18	5.00
Gd	0.86	0.90
Tb	5.34	5.78
Dy	1.05	1.18
Ho	2.86	3.26
Er	0.43	0.48
Tm	2.76	3.15
Yb	0.40	0.45
Lu	12.67	8.60
Th	6.77	6.47
$(La/Yb)_{CN}$	3.09	1.84
$(La/Sm)_{CN}$	1.51	1.13
$(Gd/Yb)_{CN}$	1.57	1.33
(Eu/Eu*)	0.95	0.95

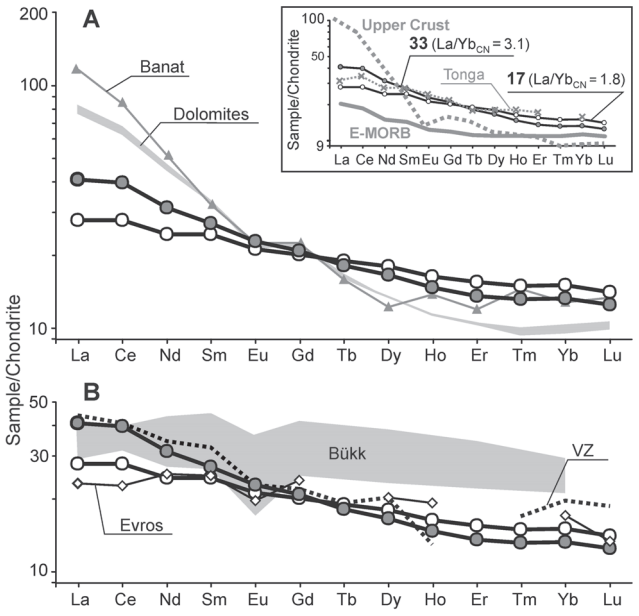

Fig. 6. Rare Earth element patterns of Bovec volcanic clasts 33 and 17 (HL and LL group, respectively) normalized to chondrite (CN; Boynton 1984). VZ = Vardar Zone. Other abbreviations and source data as in Figs. 4 and 5.

pattern (La/Sm_{CN}=3.9) given by high La/Sm_{CN} ratio (3.8 and 2.4), strongly different from the studied HL clasts (1.1–1.5).

The volcanics from Evros (La/Yb_{CN}=1.6) and Vardar Zone (La/Yb_{CN}=2.3; Fig. 6B), again show an affinity with the LL and HL samples. Bükk lavas differ by showing a flatter REE pattern, to indicate the presence of a very important N-MORB like component in their genesis (Downes et al. 1990).

Petrogenetic aspects

Multi-elemental and REE patterns emphasize that the studied volcanics have an ocean-arc type affinity and show the strongest similarities with less recrystallized metabasites from the Vardar Zone and Rhodope areas. This implies that the La/Y ratio of the clasts covers all the compositive range shown by the Jurassic arc-type magmatites. This affinity could better appear in Fig. 7 (La/Y vs. La) where all the studied clasts span from the more depleted arc-tholeiites type (Evros and Bükk, which plot close to E-MORB and the selected arc-type end-members) towards the enriched ones (Vardar Zone selected sample), which approximate an upper crustal composition for the La/Y ratio. In the TiO_2/Al_2O_3 vs. Zr/Al_2O_3 tectonomagmatic diagram (Müller et al. 1992), all the clasts fall inside the post-collisional and continental arc basalts, as well as Tonga, Evros, Vardar and Bükk selected samples (Fig. 8).

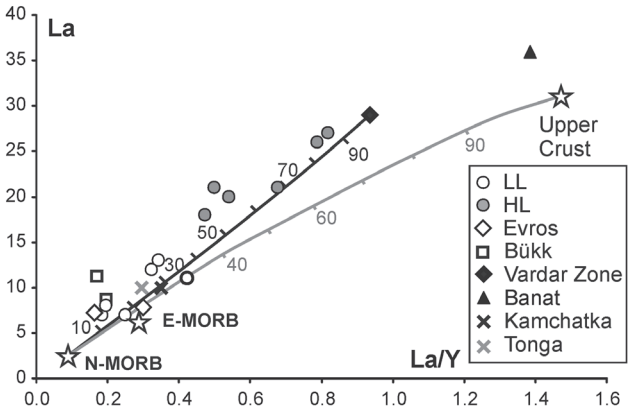

Fig. 7. La vs. La/Y diagram of Bovec volcanic clasts. The black line represents a mixing curve. Abbreviations and source data as in Figs. 4 and 5.

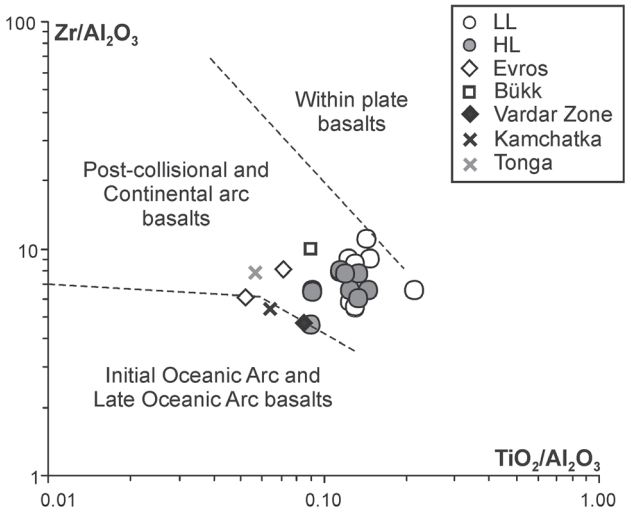

Fig. 8. Zr/Al_2O_3 vs. TiO_2/Al_2O_3 tectonomagmatic diagram (Müller et al. 1992). Abbreviations and source data as in Figs. 4 and 5.

The Kamchatka sample, which plots at the border with the oceanic arc basalts, is an exception. This suggests a fairly high TiO_2 (and Zr) content in the source able to contrast the oxide fractionation due to the high oxygen fugacity which generally characterizes arc magmatism. Moreover, in the most significative tectonomagmatic diagram of Fig. 9 (modified after Beccaluva et al. 1991), the selected clasts plot over the Tonga-Kermadec field, to suggest a petrogenetic affinity with the recent arc-type tholeiites. The higher Th/Zr ratios, shown by the depleted arc-type magmas from Evros, Bükk and Vardar, are probably due to Th mobilization during secondary metamorphic and/or hydrothermal events.

Notably, the high La/Yb_{CN} and low Th/Zr ratios of HL type clasts, not linked with the important La/Sm_{CN} increase, which characterizes the considered calc-alkaline magmas (Dolomites and Banat), suggest that the chemical differences between LL and HL clasts could not be related to contamination involving a mixing or an AFC process between LL and an upper crustal component. In fact the mixing line of Fig. 7, suggests that to increase the La/Y ratio from LL to HL groups, the involvement of about 60 wt. % of an upper crustal component would be necessary; a percentage not compatible with major elements composition. Thus, La/Y and La/Yb, as well as Th/Zr ratios seem to indicate different mantle sources characterized by different LREE and Th content for LL and HL groups. Considering the recent Vardar Jurassic arc reconstruction (Csontos & Vörös 2004) it is possible that the LL volcanic clasts could be related to the inner parts of an arc, while the HL ones could represent marginal products, situated closer to a continental plate.

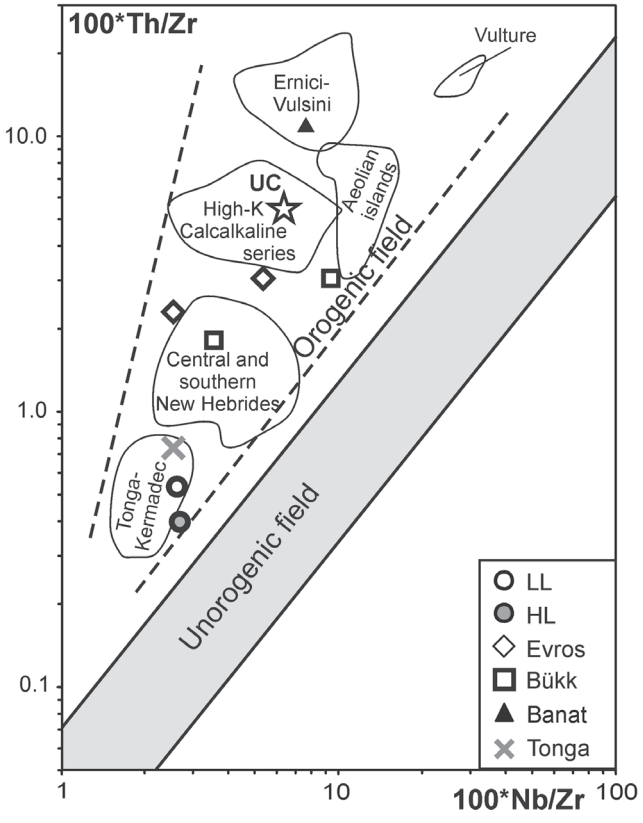

Fig. 9. 100*Th/Zr vs. 100*Nb/Zr tectonomagmatic diagram (modified after Beccaluva et al. 1991). UC = Upper Crust composition. Other abbreviations and source data as in Figs. 4 and 5.

Discussion

The Vardar Ocean was characterized from Early Jurassic to Early Cretaceous by an arc system which evolved through a movement toward the Bihor Getic–Austroalpine junction (Fig. 9 inset; modified after Csontos & Vörös 2004). The relative movements between the Bihor-Getic plate and Dinaric High Karst margin, led to Vardar Ocean closure. Thus, most of the arc-magmatic products obducted and developed into the ophiolitic complexes, mostly outcropping in the Internal Dinarides (mainly represented by Vardar Zone), Rhodope and Bükk Mountains. From the Aptian up to the end of the Maastrichtian, according to Csontos & Vörös (2004), only a portion of such magmatism seems not affected by the compressive movements, being trapped inside the core of a fold (current Vardar-Mures nappe) developed inside the Bihor-Getic platform (Fig. 10), which was probably deformed by the arc structure. Probably, during the Maastrichtian, such a structure was located fairly near the Bovec area, which represented a marginal portion of the Slovenian Basin inside the outer margin of the Pindos Sea (Fig. 10).

The studied volcanic clasts are tholeiites with a strong arc-type signature. Moreover, the studied clasts show a chemical affinity with the tholeiites from the Internal Di-

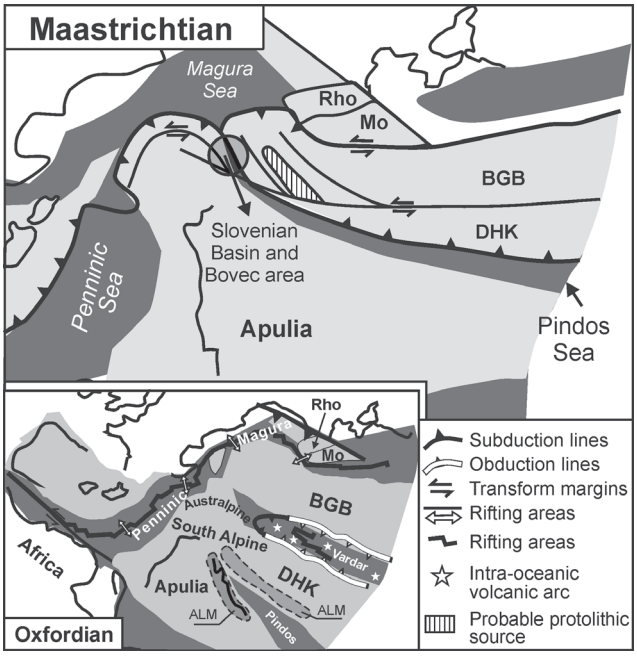

Fig. 10. Mesozoic plate reconstruction of the Carpathian region (modified after Csontos & Vörös A. 2004). BGB = Bihor-Getic block; DHK = Dinaric High Karst margin; Rho = Rhodope Mountains; Mo = Moesia; ALM = Aniso-Ladinian calc-alkaline magmatism.

narides, as well as with all the Jurassic arc magmatism of the Dinaridic-Carpathian region; however these tholeiites cannot be considered as protoliths, having probably metamorphosed during obduction and being located someway from the Bovec area, as is suggested by the homogeneous grain size and shape shown by both the clast groups and by their comparable grade of alteration which, indeed, indicate a very close provenance. The protolithic rocks probably belonged to the Vardar arc system, but the LL and HL groups show chemical features not related to simple fractional crystallization, and imply significative differences in the source composition of the protolithic rocks. Notably, different magmatic sources have also been proposed by Lenaz et al. (2000), through the chemistry of the Julian Basin flysch detrital Cr-spinels. Moreover, Lenaz et al. (2000, 2003) suggested that this spinel detritus is related to the Vardar Ocean closure.

In the authors' opinion an important role has been played by the fold (probably arc-driven) located within the Bihor-Getic plate, where different portions of unmetamorphosed magmatic arc-type lavas were approaching.

Acknowledgments: The authors would like to thank Miss Christine Smith for the revision of English text and Mr Lorenzo Furlan for thin sections.

References

Aubouin J. 1963: Essai sur la paléogeographie post-triasique et l'évolution secondaire et tertieire du versant sud des Alpes orientales (Alpes méridionales; Lombardie et Vénétie, Italie; Slovénie occidentale, Yougoslavie). *Bull. Soc. Geol. France* 71, 730–766.

Beccaluva L., Digirolamo P. & Serri G. 1991: Petrogenesis and tectonic setting of the Roman Volcanic Province, Italy. *Lithos* 26, 191–221.

Bellieni G., Piccirillo E.M. & Zanettin B. 1981: Classification and nomenclature of basalts. *I.U.G.S. subcommissions on the systematics of igneous rocks. Circular 34, Contribution n. 86,* 1–19.

Boynton W.V. 1984: Cosmochemistry of the rare Earth elements: meteorite studies. In: Henderson P. (Ed.): Rare Earth element geochemistry. *Elsevier*, Amsterdam, 63–114.

Brown G.M. & Vincent E.A. 1963: Pyroxenes from the late stages of fractionation of the Skaergaard Intrusion, East Greenland. *J. Petrology* 4, 175–197.

Buser S. 1986a: Geological map of SFRJ 1:100,000. Sheets Tolmin and Videm (Udine). *Geol. Zavod,* Beograd, 1–103.

Buser S. 1986b: Geological map of SFRJ 1:100,000 Sheets Tolmin and Videm (Udine). Explanatory text. *Zvezni Geol. Zavod,* Beograd, 1–103.

Cousin M. 1970: Esquisse géologique des confins italo-yougoslaves: leur place dans les Dinarides et les Alpes méridionales. *Boll. Soc. Geol. France* 7, XII, 6, 1034–1047.

Csontos L. & Vörös A. 2004: Mesozoic plate tectonic reconstruction of the Carpathian region. *Palaeogeogr. Palaeoclimatol. Palaeoecol.* 210, 1–56.

De La Roche H., Leterrier P., Grandclaude P. & Marchal M. 1980: A classification of volcanic and plutonic rocks using R1-R2 diagram and major-element analysis. Its relationships with current nomenclature. *Chem. Geol. 29,* 183–210.

De Min A., Piccirillo E.M., Marzoli A., Bellini G., Renne P.R., Ernesto M. & Marques L.S. 2003: The Central Atlantic Magmatic Province (CAMP) in Brazil: Petrology, geochemistry, $^{40}Ar/^{39}Ar$ ages, paleomagnetism and geodynamic implications. In: Hames W.E., McHone J.G., Renne P.R. & Ruppel C. (Eds.): The Central Atlantic Magmatic Province: Insights from fragments of Pangea. *AGU, Geophys. Monograph,* 136.

Downes H., Pantó GY., Arcai P. & Thirlwall M.F. 1990: Petrology and geochemistry of Mesozoic igneous rocks, Bükk mountains, Hungary. *Lithos* 24, 201–215.

Dupont A., Vander Auwera J., Pin C., Marincea Ş. & Berza T. 2002: Trace element and isotope (Sr, Nd) geochemistry of porphyry- and skarn-mineralising Late Cretaceous intrusions from Banat, western South Carpathians, Romania. *Mineral. Deposita* 37, 568–586.

Gill J.B. 1976: Composition and age of Lau Basin and ridge volcanic rocks: implications for evolution of interarc basin and remnant arc. *Bull. Geol. Soc. Amer.* 87, 1384–1395.

Govindaraju K. & Mevelle G. 1987: Fully automated dissolution and separation methods for inductively coupled plasma atomic emission spectrometry rock analysis: application to the determination of rare earth elements. *J. Analytical Atomic Spectrometry* 2, 615–621.

Kersting A.B. & Arculus R.J. 1994: Klyuchevskoy volcano, Kamchatka, Russia: the role of high-flux recharged, tapped and fractionated magma chamber(s) in the genesis of high-Al_2O_3 from high-MgO basalt. *J. Petrology* 35, 1–41.

Kretz R. 1982: Transfer and exchange equilibria in a portion of pyroxene quadrilater as deduced from natural and experimental data. *Geochim. Cosmochim. Acta* 46, 411–421.

Kudo A.M. & Weill D.F. 1970: An igneous plagioclase thermometer. *Contr. Mineral. Petrology* 25, 52–65.

Kuščer D., Grad K., Nosan A. & Ogorelec B. 1974: Geology of the Soca Valley between Bovec and Kobarid. *Geologija* 17, 425–476.

Le Bas M.J., Le Maitre R.W., Streckeisen A. & Zanettin B. 1986: A chemical classification of volcanic rock based on the total alkali-silica diagram. *J. Petrology* 27, 745–750.

Lenaz D., Kamenetsky V.S., Crawford A.J. & Princivalle F. 2000: Melt inclusions in detrital spinel from the SE Alps (Italy-Slovenia): a new approach to provenance studies of sedimentary basin. *Contr. Mineral. Petrology* 139, 748–758.

Lenaz D., Kamenetsky V.S. & Princivalle F. 2003: Cr-spinel supply in the Brkini, Istrian and Krk Island flysch basins (Slovenia, Italy and Croatia). *Geol. Mag.* 140, 335–342.

Magganas A.C. 2002: Constraints on the petrogenesis of Evros ophiolite extrusives, NE Greece. *Lithos* 65, 165–182.

McDonough W.F. & Sun S. 1995: The composition of the Earth. *Chem. Geol.* 120, 223–253.

Miyashiro A. 1974: Volcanic rock series in island arcs and active continental margins. *Amer. J. Sci.* 274, 321–355.

Müller D., Rock N.M.S. & Groves D.I. 1992: Geochemical discrimination between shoshonitic and potassic volcanic rocks in different tectonic settings: a pilot study. *Miner. Petrology* 46, 259–289.

Mutti E., Tinterri R., Benevelli G., di Biase D. & Cavanna G. 2003: Deltaic, mixed and turbidite sedimentation of ancient foreland basins. *Mar. Petrol. Geol.* 20, 733–755.

Ogorelec B., Šribar L. & Buser S. 1976: On lithology and biostratigraphy of Volče limestone. *Geologija* 19, 126–151.

Pamić J., Tomljenović B. & Balen D. 2002: Geodynamics and petrogenetic evolution of Alpine ophiolites from the Central and NW Dinarides: an overview. *Lithos* 65, 113–142.

Papike J.J., Cameron K.L. & Baldwin K. 1974: Amphiboles and pyroxenes. Characterisation of other than quadrilateral components and estimates of ferric iron from microprobe data. *Geol. Soc. Amer. – Abstract with Program* 6, 1053–1054.

Pavšič J. 1994: Biostratigraphy of Cretaceous, Paleocene and Eocene clasties of Slovenia. *Razprave IV. razr., SAZV* 35, 65–84.

Rosset A., Lenaz D., Tunis G., De Min A. & Tosone A. 2003: Preliminary characterization of magmatic clasts from conglomerate within the Bovec flysch (Slovenia). *Ann. Ser. Hist. Natur.* 13, 257–262.

Rudnick R.L. & Gao S. 2004: Composition of continental crust. In: Holland H.D. & Turekian K.K. (Eds.): Treatise on geochemistry. *Elsevier*, V. 3 (The Crust), 1–64.

Selli R. 1947: Geology of High Isonzo Basin (stratigraphy and tectonics) in Italian. *Giorn. Geol.* 2a, 19, 1–153.

Sun S. & McDonough W.F. 1989: Chemical and isotopic systematics of oceanic basalts: implications for mantle composition and processes. In: Saunders A.D. & Norry M.J. (Eds.): Magmatism in the Ocean Basin, special publication. *Geol. Soc. London* 42, 313–345.

Venturini S. & Tunis G. 1992: Composition of Cenozoic conglomerates of Friuli: preliminary data. *Studi Geologici Camerti*, *Spec. Vol.* 1992, 2, 285–295 (in Italian).